Journal of Achievements in Materials and Manufacturing Engineering
VOLUME 54
ISSUE 2
October
2012

Dilatometric examination of continuously heated austenite formation in hypoeutectoid steels

B. Pawłowski*
Faculty of Metals Engineering and Industrial Computer Science, AGH University of Science and Technology, Al. Mickiewicza 30, 30-059 Kraków, Poland
* Corresponding e-mail address: bpawlow@agh.edu.pl

Received 03.08.2012; published in revised form 01.10.2012

Materials

ABSTRACT

Purpose: of this work is to present possibility of proper determination of pearlite dissolution finish temperature Ac_{1f} during heating of hypoeutoctoid steels.
Design/methodology/approach: The presented schemes of splitting the first derivative curve of hypoeutectoid steels dilatograms are based on experimental dilatograms and their first derivatives obtained by use of the dilatometric technique.
Findings: The nine possible schemes of splitting the first derivative curve of hypoeutectoid steels dilatograms were developed. These schemes have been developed for three main cases: ferrite to austenite transformation temperature range is wider than for pearlite to austenite transformation, ferrite to austenite transformation temperature range has the same width as for the pearlite to austenite transformation and ferrite to austenite transformation temperature range is shorter than for pearlite to austenite transformation. Presented schemes are fully compatible with experimental results.
Research limitations/implications: Further verification of correctness of the presented schemes and the development of appropriate curve fitting software is needed.
Practical implications: Broadening the knowledge on the phase transformation kinetics of hypoeutectoid steels during heating. The basics for the automate process of determination of critical temperatures in steels, especially the Ac_{1f} temperature, were established.
Originality/value: The originally schemes of splitting the first derivative curve of hypoeutectoid steels dilatograms were developed.
Keywords: Critical temperatures in steel; Phase transformation; Heating dilatogram; Pearlite dissolution finish temperature

Reference to this paper should be given in the following way:
B. Pawłowski, Dilatometric examination of continuously heated austenite formation in hypoeutectoid steels, Journal of Achievements in Materials and Manufacturing Engineering 54/2 (2012) 185-193.

1. Introduction

The austenite formation in hypoeutectoid steels during continuous heating consists of two phenomena: pearlite dissolution and proeutectoid ferrite to austenite transformation. In this work austenite formation start temperature on heating will be described as Ac_{1s} (s = start), according to Wever and Rose nomenclature Ac_{1b} (where b = beginn) [1]. Similarly, pearlite to austenite

transformation finish temperature will be described as Ac_{1f} (f = finish, Wever and Rose nomenclature Ac_{1e}, where e = ende). Such split of the A_1 transformation temperature during heating (and cooling) of steels (hypoeutectoid, eutectoid and hypereutectoid) is because in steels, contrary to the iron-carbon binary system, eutectoid transformation does not take place at constant temperature (according to the Gibbs' phase rule for binary system the number of degrees of freedom for eutectoid transformation is equal zero) but at certain temperature range. Austenite formation start temperature used to be marked as Ac_1 (here Ac_{1s}) but there is no uniform description for pearlite to austenite transformation finish temperature (here Ac_{1f}). Only a few authors use the description Ac_{1s} and Ac_{1f} (or, according to Wever and Rose, Ac_{1b} and Ac_{1e}) [2-9]. Pearlite dissolution start and finish temperature (A_1 transformation start and finish temperature in steels on heating) are described in many different ways, as it is presented in Table 1.

Table 1.
Different descriptions of Ac_{1s} and Ac_{1f} temperature

Ac_{1s} temperature	Ac_{1f} temperature	source
A_1(L) (L – lower temperature)	A_1(U) (U – upper temperature)	[10]
A_1^-	A_1^+	[11]
Ac_1	Af (f – finish temperature)	[12]
Ac_1	Ac_ρ	[13]
Ac_1	T_C	[14]
Ac_1	Ac_1'	[15]
Ac_1	Af_1 (f – finish temperature)	[16]
Ac_1	A_{pf} (pf – pearlite finish)	[17]

Similarly to the pearlite to austenite transformation finish temperature, there is no uniform notation for austenite to pearlite transformation start temperature on cooling (according to the nomenclature used in this paper, this temperature should be marked as Ar_{1s}). Thus, this temperature is marked, for example, as Ar' [18], T_P [19], T_f^F [20], T_{A_1} [21] or T_E^S [22].

The Ac_{1f} temperature determines the start of the coexistence range of ferrite and austenite during heating as well as the temperature determining the finish of this range, during cooling, in hypoeutectoid steels. The accurate determination of this coexistence range of ferrite and austenite (i.e. determination of temperatures Ac_{1f} and Ac_3, so-called – among others – critical points or critical temperatures) is of great importance in the industrial heat treatment of newer types of sheet steels, such as DP (Dual Phase) and TRIP (Transformation Induced Plasticity) steels, which were designed to pass through α+γ phase field (intercritical annealing region), with the austenite transforming to martensite on subsequent cooling to room temperature [23]. The amount of austenite within matrix microstructures of ferrite grains depends strongly on temperature of annealing, which should be between Ac_{1f} and Ac_3 temperatures. DP and TRIP steels are widely used in the automobile industry for their superior mechanical properties [23].

Approaches for predicting pearlite to austenite transformation start and finish temperatures Ac_{1s} and Ac_{1f} (as well as austenite formation finish temperature Ac_3) during heating was made by regressing experimentally determined critical temperatures with respect to the steel chemistry (Eq.1, where Ac_1 means Ac_{1s} [25]) and by use of an artificial neural network method [9, 24, 25].

$$Ac_1\ [^oC] = 739–22.8\cdot C–6.8\cdot Mn+18.2\cdot Si +11.7\cdot Cr–15\cdot Ni-6.4\cdot Mo –5\cdot V–28\cdot Cu \quad (1)$$

An example of artificial neural network application for estimation of the Ac_1 temperature (austenite formation start temperature during heating, according to nomenclature used in this work it is Ac_{1s} temperature) is shown in Figure 1 [25]. Forecasting of critical temperatures by use of artificial neural network technology gives better agreement between predicted and experimental values than empirical relationships based on linear multiple regression method. It is due to the synergistics effect of alloying elements on phase transformation in steels [25].

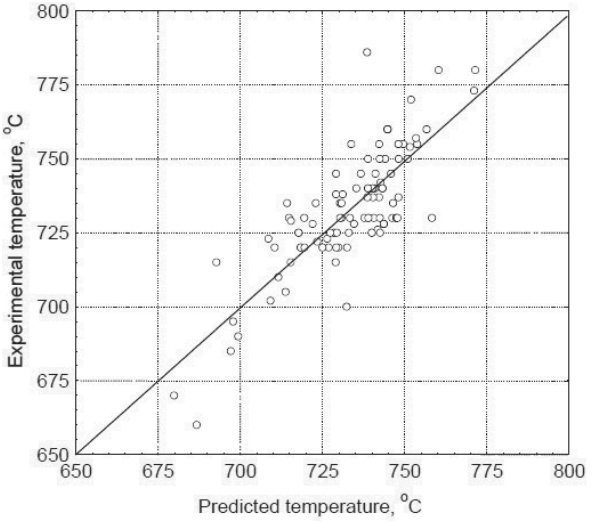

Fig. 1. Comparison of the experimental Ac_1 temperatures with values calculated using the neural network method [25]

In Ref. [25] results of predicting critical temperatures Ac_1, Ac_3, B_s and M_s by use of artificial neural network method were compared with results obtained by use of empirical relationships reported in literature. For example, Pearson correlation coefficient for the neural network model used for predicting Ac_3 temperature was equal 0.925 while for Andrews formulae (Eq. 2, [26]) Pearson correlation coefficient was 0.790 [25].

$$Ac_3\ [^oC] = 910–203\cdot\sqrt{C}–15.2\cdot Ni+44.7\cdot Si +104\cdot V+31.5\cdot Mo +13.1\cdot W \quad (2)$$

However, the best accuracy in determining the temperatures of austenite formation during continuous heating (as well as other critical temperatures) is obtained using dilatometric method. As stated in Ref. 28, dilatometry is believed to be the best current method for development of data in support of distortion and residual stress predictions because it measures both, phase

transformation kinetics and thermal strains. Nowadays ultra high resolution dilatometers have resolution even up to nanometres (laser dilatometer built after the Michelson-Interferometer principle) [27]. In many cases, especially for proper determination of critical points, such ultra high resolution is not necessary, but sometimes low resolution dilatometric experiments results do not show very small volume changes caused by some phase transformation, as it will be discussed later.

2. Dilatometric examinations

The start temperature of pearlite to austenite transformation (Ac_1 temperature) and austenite formation finish temperature (Ac_3 temperature) is easy to determine by dilatometric analysis, as it is shown in Figure 2 [28]. Both critical temperatures can be determined from changes in the slope of a strain versus temperature plot. Determination of the critical temperatures from the dilatometric curve is conducted considering that Ac_1 corresponds to the temperature at which the expansion deviates from a linear behaviour during heating and the sample starts to contract due to the austenite formation; whereas Ac_3 is the temperature at which expansion begins again to depend linearly on temperature once the sample is fully austenitic [29].

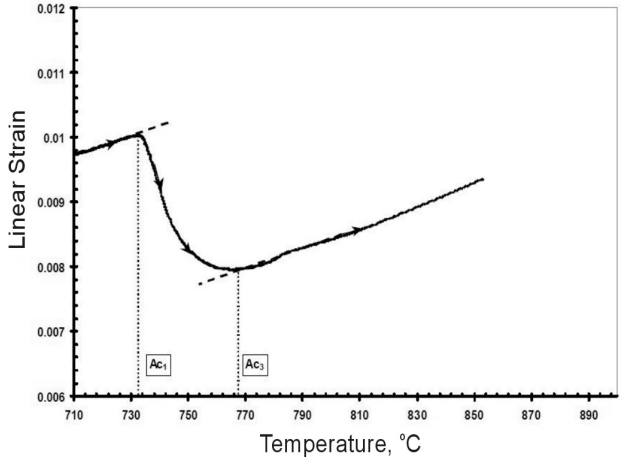

Fig. 2. Dilation strain versus temperature showing determination of Ac_1 and Ac_3 temperatures [28]

Since Ac_1 and Ac_3 temperatures are sensitive to heating rate [29-31], the heating rate employed should be noted. According to [28], during the determination of the critical temperatures Ac_1 and Ac_3, the thermal cycle to be used is to heat the test specimen to 700°C, ± 5°C, at a nominal rate of 10°C/s. Heating must then be continued at a nominal rate of 28° Celsius per hour (~0.008°C/s) while strain is continuously measured until the Ac_1 and Ac_3 temperatures are identified.

It should be noted here, that although critical temperatures are sensitive to heating rate (transformation temperatures increase with heating rate) the Ac_1 temperature is near the equilibrium temperature Ae_1 (calculated with Thermo-Calc [31]) for a 0.3°C/s heating rate as it shown in Figure 3. It can be observed that the increasing heating rate has a greater effect on Ac_3 than on Ac_1 temperature and the transformation temperatures are higher for ferrite-pearlite microstructure (hot rolled steel) than for tempered martensite microstructure (quenched and tempered steel) in all cases. Temperature differences between hot rolled and quenched and tempered initial states of tested AISI 5150 steel increases also with increasing heating rate, as it is presented in Figure 4 [31].

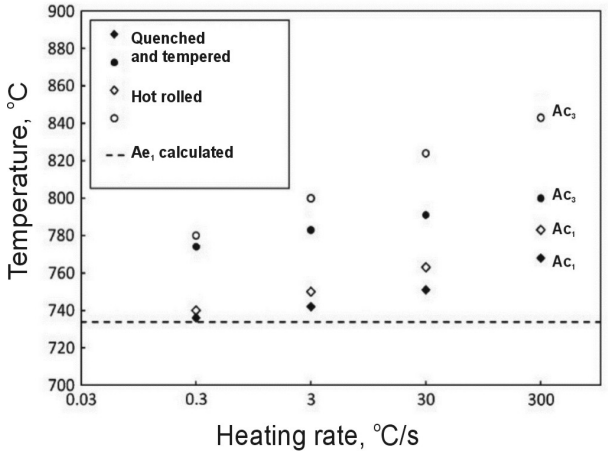

Fig. 3. The Ac_1 and Ac_3 temperatures from dilatometric measurements with different heating rates and calculated Ae_1 temperature (dashed line) for AISI 5150 steel [31]

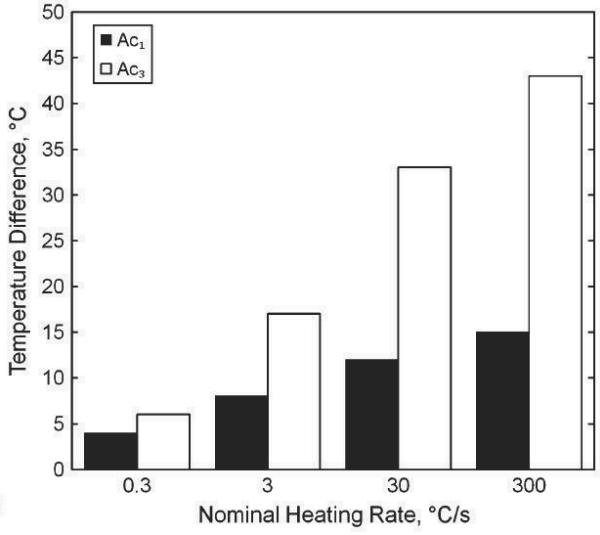

Fig. 4. Temperature differences (hot rolled – quenched and tempered initial state) for Ac_1 and Ac_3 temperatures for AISI 5150 steel [31]

Similar effect of heating rate on critical temperatures of low carbon microalloyed steel was also previously reported in Refs. [29, 32]. Experimental Ac_{1s} (originally marked as Ac_1) and Ac_3 temperatures, as well as Ac_{1f} temperatures (originally marked as Ac_ρ) for four different heating rates are shown in Table 2 (eight different dilatometric curves were analysed by the cited authors for the each heating rate in order to determine these temperatures.

Table 2.
Experimental Ac_{1s} and Ac_3 temperatures, as well as Ac_{1f} temperatures for four different heating rates [29, 32]

Heating rate, °C/s	Ac_{1s}, °C	Ac_{1f}, °C	Ac_3, °C
0.05	732 ± 1	756 ± 4	893 ± 4
0.5	736 ± 2	756 ± 2	889 ± 6
5	742 ± 2	763 ± 2	897 ± 5
10	752 ± 4	776 ± 5	905 ± 5

Figure 5 shows dilatometric curve, after continuous heating at 0.05°C/s, where the pearlite to austenite transformation finish temperature Ac_{1f} is marked as Ac_ρ.

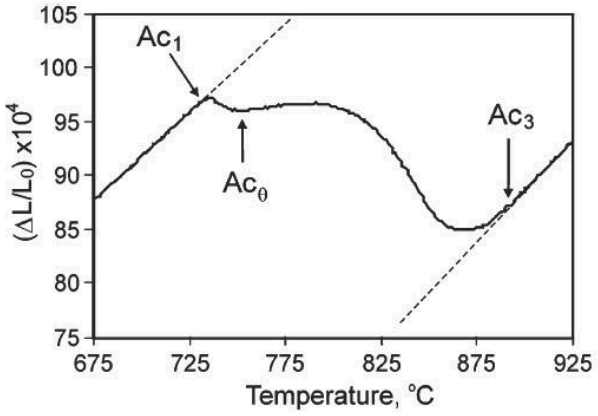

Fig. 5. The dilatometric curve of low carbon microalloyed steel after heating at 0.05°C/s [29, 32]

As stated in Refs. [29, 32], Ac_{1f} (oryginally Ac_ρ) temperature is the temperature at which the first contraction on the dilatometric curve due to the pearlite to austenite transformation finishes. This temperature is less evident to see from the curve $\Delta L/L_0$ versus temperature, but easier to determine from the first derivative as it is shown in Figure 6 [29].

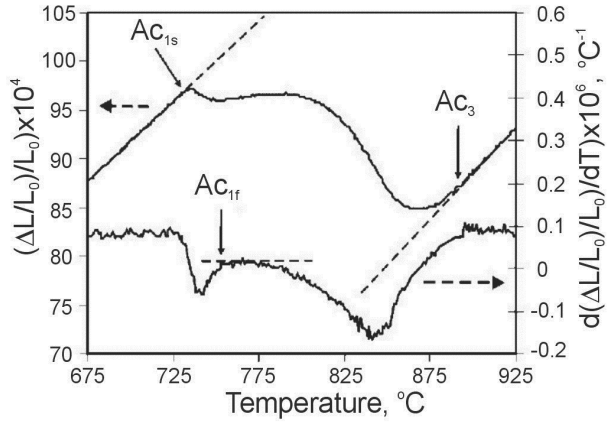

Fig. 6. The dilatometric curve of low carbon microalloyed steel after heating at 0.05°C/s and its derivative [29]

In some cases, the first contraction (due to the pearlite to austenite transformation) on the dilatometric curve of hypoeutectoid steel during heating (at 0.05°C/s) is not observed as it is shown in Figure 7 [33], presenting dilatometric examination of C55 carbon steel (which microstructure consists of pearlite with very small amount of proeutectoid ferrite, sample after normalizing annealing), performed at the Laboratory of Phase Transformations, Department of Physical and Powder Metallurgy, AGH University of Science and Technology, by use of the Adamel Lhomargy DT1000 dilatometer, the same type of dilatometer as used in Refs. [29, 32]. As it is shown, determination of pearlite dissolution finish temperature is not possible neither on the dilatometric curve nor on its derivative. Only the pearlite to austenite transformation start temperature (Ac_{1s} temperature) and the austenite formation during heating end temperature (Ac_3 temperature) can be determined.

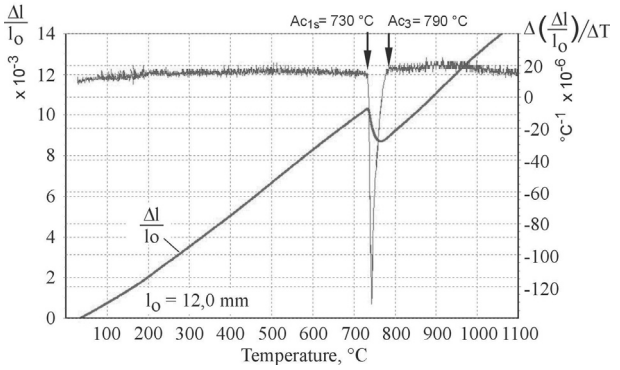

Fig. 7. The dilatometric curve of C55 carbon steel after heating at 0.05°C/s and its derivative (DT1000 dilatometer) [33]

Additional dilatometric examinations during heating of the same C55 carbon steel were performed by use of ultra high resolution Linseis L78 RITA (Rapid Induction Thermal Analysis). The sample of C55 steel, prior to the dilatometric examinations, was normalizing annealed the same way as sample tested by use of DT1000 dilatometer. The obtained dilatogram and its derivative is presented in Figure 8.

By use of a L78 RITA dilatometer, the pearlite to austenite transformation end temperature can be easily estimated from the derivative curve, as it is shown in Figure 8. The L78 RITA dilatometer is characterised by a much better resolution than the DT1000 dilatometer and this enables the determination of a Ac_{1f} temperature, although only from the derivative curve. On the dilatometric curve contraction due to the pearlite to austenite transformation is not clearly observed just as it was in case of examination by use of the DT1000 dilatometer (compare Fig. 7 and Fig. 8). It is rather puzzling, that in the case of C55 steel (containing very small amount of ferrite) the effect related to the finish of the pearlite transformation appears on the left slope of a V-shaped derivative curve but almost identical derivative curve was obtained after heating of Mn-Co steel (Fig. 9) containing also high amount of pearlite in pearlie-ferritic microstructure.

As it was mentioned above the austenite formation in hypoeutectoid steels during continuous heating consists of two phenomena: pearlite dissolution and proeutectoid ferrite to austenite transformation. Both this phase transformation result in contraction on the dilatometric curve.

The analysis of the dilatograms and its derivatives obtained over many years at the Laboratory of Phase Transformations (by use of high resolution dilatometer DT1000 and ultra high resolution dilatometer L78 RITA) led to the development of nine possible schemes of split of the derivative curves of hypoeutectoid steels heating dilatograms in temperature range between Ac_{1s} and Ac_3 [35].

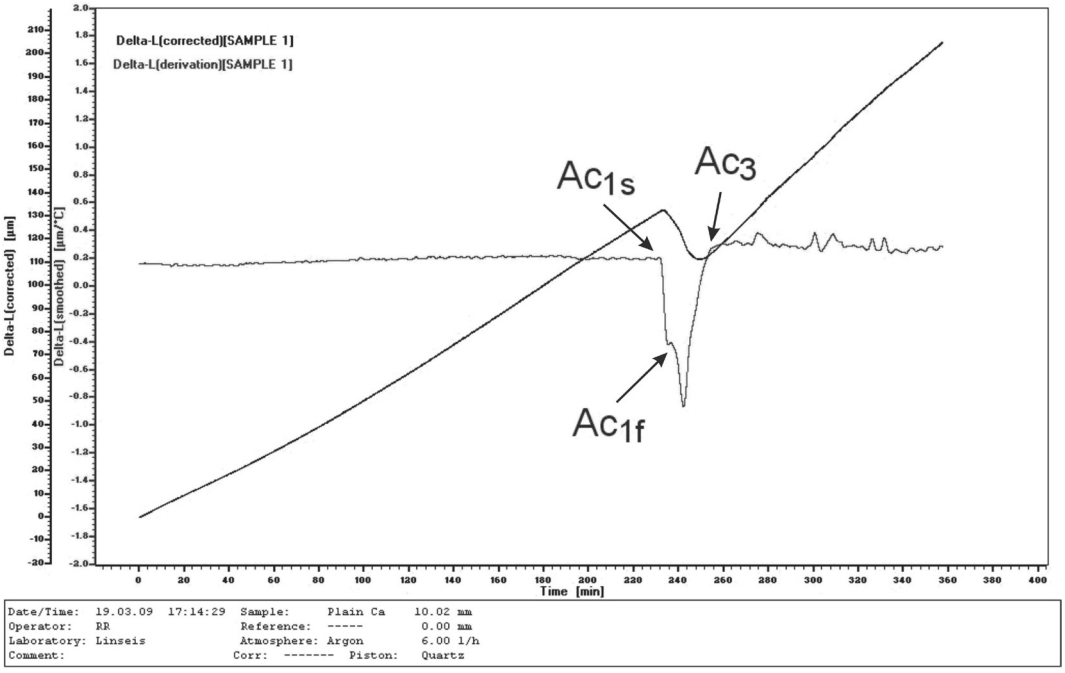

Fig. 8. The dilatometric curve of C55 carbon steel after heating at 0.05°C/s and its derivative (L78 RITA dilatometer) [33]

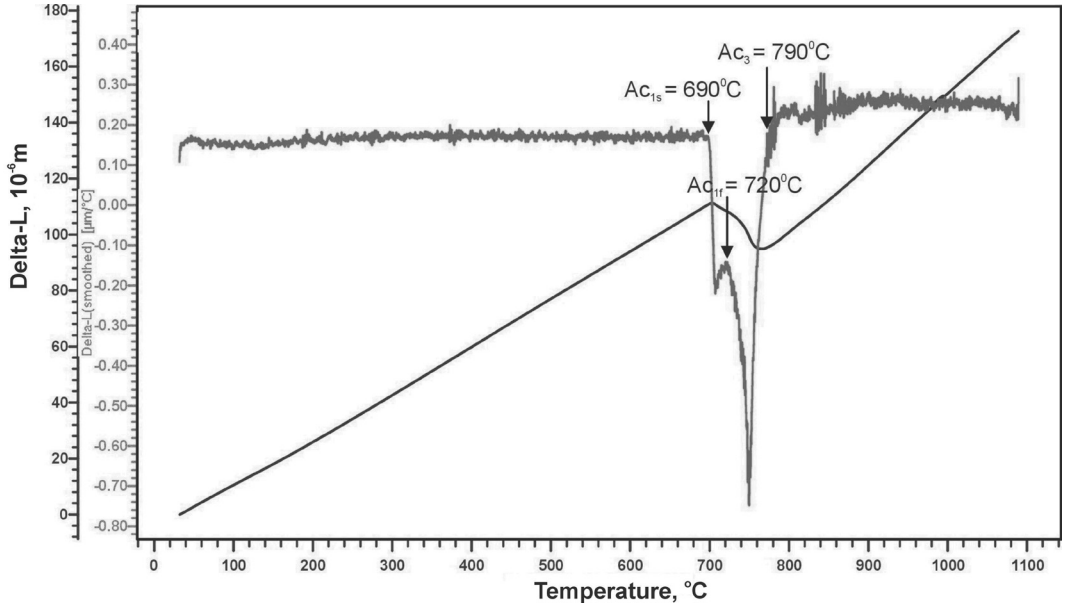

Fig. 9. The dilatometric curve of Mn-Co steel with high amount of pearlite after heating at 0.05°C/s and its derivative (L78 RITA dilatometer) [34]

3. A split of derivative of hypoeutectoid steels heating dilatograms

Observed in dilatometric heating curves of hypoeutectoid steels effect of volume contraction between Ac_{1s} and Ac_3 temperatures could be divided into two separate but overlapping phenomena: a contraction due to pearlite to austenite formation and a contraction caused by ferrite to austenite transformation.

The first derivative of dilatometric curve at this temperature range shows effect of volume contraction more accurately and this effect could be divided into two separate phenomena as it is shown in Figure 10 [35].

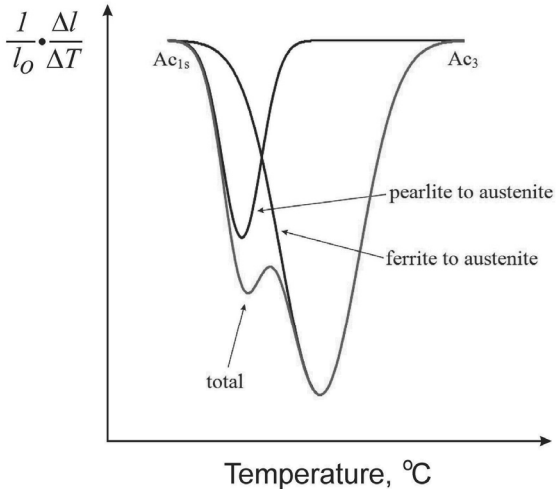

Fig. 10. Derivative of heating dilatogram (between Ac_{1s} and Ac_3) of hypoeutectoid steel splitted into two component curves [35]

The magnitude of contraction in derivative components represent the maximum transformation rate and these component curves may be expressed mathematically as follows:

- pearlite to austenite transformation component

$$\Delta\left(\Delta l / l_0\right)/\Delta T = 1 - \alpha_P \cdot e^{-\beta_P T^2} \tag{3}$$

- ferrite to austenite transformation component

$$\Delta\left(\Delta l / l_0\right)/\Delta T = 1 - \alpha_F \cdot e^{-\beta_F (T-D)^2} \tag{4}$$

where:
T – temperature,
α_P, α_F – coefficient proportional to the transformation rate,
β_P, β_F – coefficient proportional to the transformation range,
D – temperature shift of $\alpha\rightarrow\gamma$ vs. pearlite$\rightarrow\gamma$ transformation.

The nine possible schemes of splitting the first derivative curve of hypoeutectoid steels dilatograms are presented in Figure 11. These schemes have been developed for three main cases: ferrite to austenite transformation temperature range is wider than for pearlite to austenite transformation ($\beta_F > \beta_P$ for scheme I, II, III), ferrite to austenite transformation temperature range has the same width as for the pearlite to austenite transformation ($\beta_F = \beta_P$ for scheme IV, V, VI) and ferrite to austenite transformation temperature range is shorter than for pearlite to austenite transformation ($\beta_F < \beta_P$ for scheme VII, VIII, IX). The ferrite to austenite maximum transformation rate is respectively higher ($\alpha_F > \alpha_P$ for scheme I, IV and VII), equal ($\alpha_F = \alpha_P$ for scheme II, V and VIII) and lower ($\alpha_F < \alpha_P$ for scheme III, VI and IX) than maximum rate of pearlite to austenite transformation (Table 3).

For all developed schemes additional assumption was made: the ferrite to austenite transformation start temperature is more or less higher than pearlite to austenite transformation start temperature but well below pearlite to austenite transformation start temperature. This assumption is justified by the results of scanning electron microscopy examinations presented, among others, in Refs. [29, 36], showing that during heating austenite nucleation takes place both at pearlite colonies and at ferrite/ferrite grain boundaries.

The schemes I-IX can be slightly modified as a result of the ferrite to austenite start temperature shifting to a higher temperature, but this does not change substantially their appearance, which coincides with the experimental results obtained over many years at the Laboratory of Phase Transformations AGH and cited in the literature. Examples of such modified schemes are presented in Ref. [37].

4. Conclusions

As it was mentioned above, presented schemes are fully compatible with experimental results. Dilatograms and their derivative curves presented in Figure 8 and Figure 9 corresponds with scheme IV and VII where maximum ferrite to austenite transformation rate is higer than maximum pearlite dissolution rate (column $\alpha_F > \alpha_P$ in Table 3). Experimental dilatogram compatible with scheme V or scheme VIII (column $\alpha_F = \alpha_P$ in Table 3) and dilatogram compatible with scheme III or scheme VI (column $\alpha_F < \alpha_P$ in Table 3) are presented in Figures 12 and 13.

Table 3.
The nine possible schemes of splitting the first derivative curve of hypoeutectoid steels dilatograms

Transformation range	Maximum transformation rate		
	$\alpha_F > \alpha_P$	$\alpha_F = \alpha_P$	$\alpha_F < \alpha_P$
$\beta_F > \beta_P$	scheme I	scheme II	scheme III
$\beta_F = \beta_P$	scheme IV	scheme V	scheme VI
$\beta_F < \beta_P$	scheme VII	scheme VIII	scheme IX

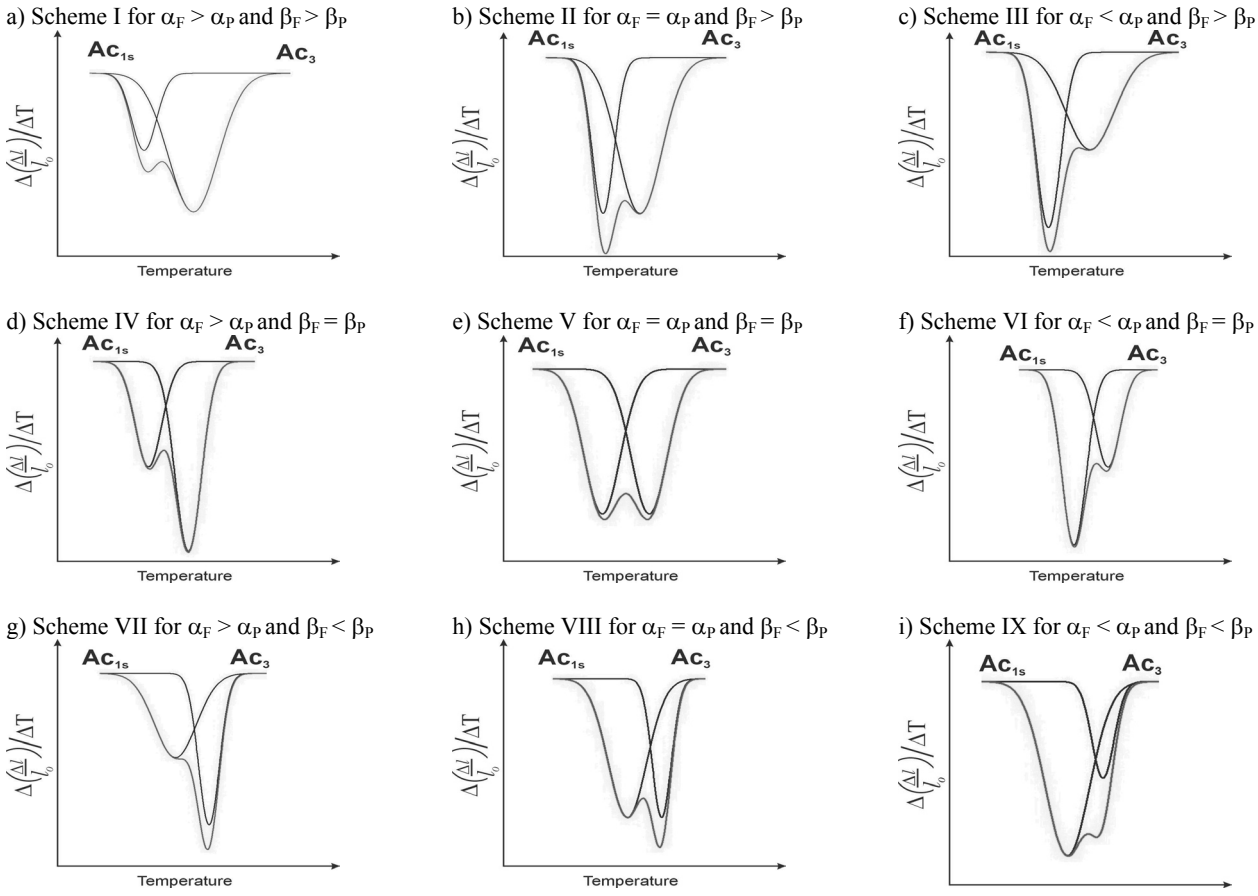

Fig. 11. Nine possible schemes of splitting the first derivative curve of hypoeutectoid steels dilatograms

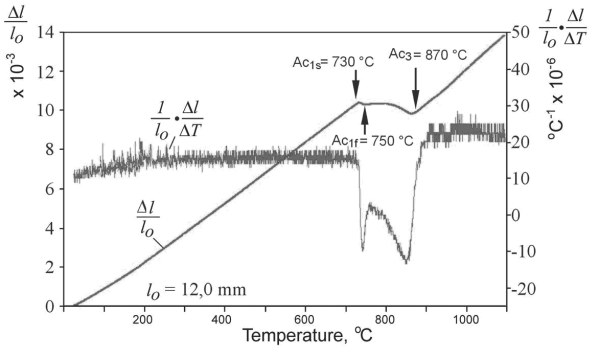

Fig. 12. Experimental dilatogram and its derivative compatible with scheme V or scheme VIII (column $\alpha_F = \alpha_P$ in Table 3) [35]

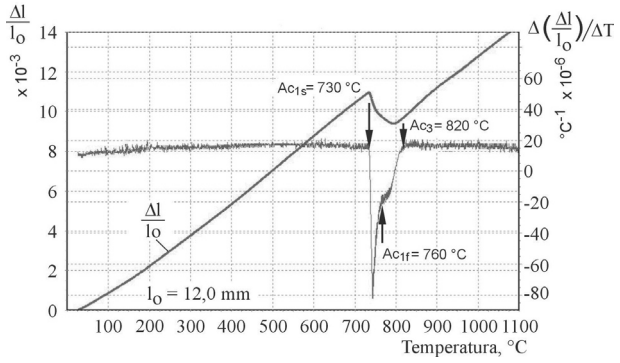

Fig. 13. Experimental dilatogram and its derivative compatible with scheme III or scheme VI (column $\alpha_F < \alpha_P$ in Table 3) [35]

Assuming correctness of presented schemes and idea of splitting the derivative curve it can be concluded that the temperatures Ac_{1f} determined in the manner presented in Figures 6, 8, 9, 12 and 13 are set incorrectly, with a greater or lesser error (see Figure 14).

Such that error in determining Ac_{1f} temperature is not significantly important for the proper planning of the heat treatment conditions in industrial practice. The Ac_{1f} temperatures are determined by use continuous heating dilatograms while industrial heat treatment consists mostly of annealing (austenitizing) at

constant temperature and as it known [38] the transformation end temperature decreases monotonically with increasing annealing time.

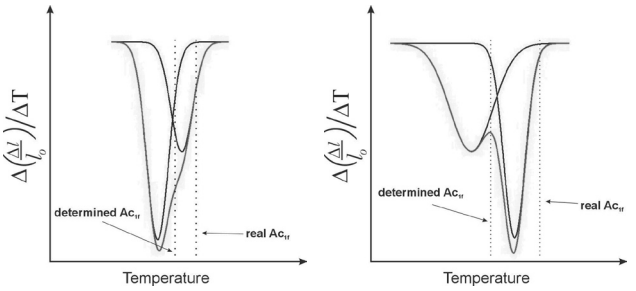

Fig. 14. Examples of possible errors in determination of Ac_{1f} temperature

Further verification of correctness of the presented schemes and the development of appropriate curve fitting software can lead to automate the process of determination of critical temperatures in steels, especially the Ac_{1f} temperature.

References

[1] F. Wever, A. Rose, Atlas zur Wärmebehandlung des Stähle, Verlag Stahleisen M.B.H., Düsseldorf (1954/56/58) (in German).

[2] H. Surm, O. Kessler, M. Hunkel, F. Hoffmann, P. Mayr, Modelling of the ferrite/carbide → austenite transformation of hypoeutectoid and hypereutectoid steels, Journal of Physics 120 (2004) 111-119.

[3] H. Surm, O. Kessler, F. Hoffmann, H.-W. Zoch, Modelling of austenitising with no-constant heating rate in hypereutectoid steels, International Journal of Microstructure and Material Properties 3/1 (2008) 35-48.

[4] J.G. Zhang, D.S. Sun, H.S. Shi, H.B. Xu, J.S. Wu, X.F. Wu, Microstructure and continuous cooling transformation thermograms of spray formed GCr15 steel, Materials Science and Engineering A 236 (2002) 20-25.

[5] F. Yan, H. Shi, B. Jin, J. Fan, Z. Xu, Microstructure evaluation during hot rolling and heat treatment of the spray formed Vanadis 4 cold work steel, Materials Characterization 59 (2008) 1007-1014.

[6] AISI A2 Cold work tool steel, Uddeholm Tooling AB, http://www.bucorp.com/files/aisi_a2.pdf [05.06.2012].

[7] J. Krawczyk, B. Pawłowski, P. Bała, Kinetics of phase transformations of undercooled austenite in 18CrNiMo7-6 steels applied for toothed wheels, Archives of Foundry Engineering 10/3 (2010) 29-34.

[8] W. Sitek, Methodology of high-speed steels design using the artificial intelligence tools, Journal of Achievements in Materials and Manufacturing Engineering 39/2 (2010) 115-160.

[9] B. Pawłowski, Critical points of hypoeutectoid steel – prediction of the pearlite dissolution finish temperature Ac_{1f}, Journal of Achievements in Materials and Manufacturing Engineering 49/2 (2011) 331-337.

[10] J.D. Verhoeven, Steel Metallurgy for the Non-Metallurgist, ASM International, Metals Park Ohio, 2007.

[11] N.H. van Dijk, S.E. Offerman, J.C.P. Klaasse, J. Sietsma, S. van der Zwaag, High-temperature magnetisation measurements on the pearlite transformation kinetics in nearly eutectoid steel, Journal of Magnetism and Magnetic Materials 268 (2004) 40-48.

[12] F.L.G. Oliveira, M.S. Andrade, A.B. Cota, Kinetics of austenite formation during continuous heating in a low carbon steel, Materials Characterization 58 (2007) 256-261.

[13] D. San Martín, P.E.J. Rivera-Díaz-del Castillo, C. García-de-Andrés, In situ study of austenite formation by dilatometry in a low carbon microalloyed steel, Scripta Materialia 58 (2008) 926-929.

[14] F.G. Caballero, C. Capdevila, C. García de Andrés, Modelling of kinetics of austenite formation in steels with different initial microstructures, ISIJ International 41/10 (2001) 1093-1102.

[15] L. Zhao, T.A. Kop, V. Rolin, J. Sietsma, A. Mertens, J. Jaques, S. van der Zwaag, Quantitative dilatometric analysis in a low-silicon TRIP steel, Journal of Materials Science 37 (2002) 1585-1591.

[16] M.Q. Macedo, A.B. Cota, F.G. da Silva Araújo, The kinetics of austenite formation at high heating rates, Revista Escola de Mines, Ouro Preto, Brasil 64/2 (2011) 163-167.

[17] S-J. Lee, K.D. Clarke, C.J. Van Tyne, A on-heating dilation conversional model for austenite formation in hypoeutectoid steels, Metallurgical and Materials Transactions 41 A (2010) 2224-2235.

[18] G.E. Totten, Steel heat treatment handbook, Second Edition, CRC Press Taylor & Francis Group, 2006.

[19] T. Garcin, S. Rivoirard, C. Elgoyhen, E. Beugnon, Experimental evidence and thermodynamics analysis of high magnetic field effects on the austenite to ferrite transformation temperature in Fe-C-Mn alloys, Acta Materialia 58 (2010) 2026-2032.

[20] S.J. Lee, M.T. Lusk, Y.K. Lee, Conversional model of transformation strain to phase fraction in low alloy steels, Acta Materialia 55 (2007) 875-882

[21] E.B. Hawbolt, B. Chau, J.K. Brimacombe, Kinetics of austenite-pearlite transformation in eutectoid carbon steel, Metallurgical Transactions 14 A (1983) 1803-1815.

[22] P. Mrvar, M. Trbižan, J. Medved, A. Križman, Study of the eutectoid transformation in the as-cast spheroidal graphite cast iron with "in situ" dilatation analysis – method for quality control, Metarials Science Forum 508 (2006) 287-294.

[23] G. Krauss, Steels. Processing, structure and performance, ASM International, Materials Park, Ohio, 2005, 221.

[24] J. Trzaska, L.A. Dobrzański, Modelling of CCT diagrams for engineering and constructional steels, Journal of Materials Processing Technology 192-193 (2007) 504-510.

[25] L.A. Dobrzański, J. Trzaska, Application of neural networks for prediction of critical values of temperatures and time of the supercooled austenite transformations, Journal of Materials Processing Technology 155-156 (2004) 1950-1955.

[26] K.W. Andrews, Empirical formulae for the calculation of some transformation temperatures, Journal of the Iron and Steel Institute 20 (1965) 721-727.

[27] Linseis Laser Dilatometer Pico-series 0,3 nm, German Patent Nr DE 103 09 284 A1, 2004.
[28] M. Mehta, T. Oakwood, Development of a Standard Methodology for the Quantitative Measurement of Steel Phase Transformation Kinetics and Dilation Strains using Dilatometric Methods (QMST), Final Report, US Department of Energy, Prepared by American Iron and Steel Institute Technology Roadmap Program, Office Pittsburgh, PA 15222, 2004.
[29] D. San Martin, T. de Cock, A. García-Junceda, F.G. Caballero, C. Capdevila, C. García de Andrés, Effect of heating rate on reaustenisation of low carbon niobium microalloyed steel, Materials Science and Technology 24/3 (2008) 266-272.
[30] F.L.G. Oliveira, M.S. Andrade, A.B. Cota, Kinetics of austenite formation during continuous heating in a low carbon steel, Materials Characterization 58 (2007) 256-261.
[31] K.D. Clarke, C.J. Van Tyne, R.E. Hackenberg, Induction hardening 5150 steel: Effects of initial microstructure and heating rate, Journal of Materials Engineering and Performance 20/2 (2011) 161-168.
[32] D. San Martin, P.E.J. Rivera-Díaz-del-Castillo, C. García de Andrés, In situ study of austenite formation by dilatometry in a low carbon microalloyed steel, Scripta Materiali 58 (2008) 926-929.
[33] B. Pawłowski, P. Bała, J. Krawczyk, Some factors influencing the determination of eutectoid start and finish temperatures in hypoeutectoid steels, Metallurgy and Foundry Engineering MaFE, AGH University of Science and Technology 35/2 (2009) 121-128.
[34] E. Rożniata, Laboratory of Phase Transformations, Department of Physical and Powder Metallurgy, AGH University of Science and Technology, Cracow, 2012 (unpublished work).
[35] B. Pawłowski, P. Bała, A new interpretation of dilatometric examinations results of hypoeutectoid steels, 2012 (submitted for publication).
[36] V.I. Savran, Y. Van Leeuwen, D.N. Hanlon, C. Kwakernaak, W.G. Sloof, J. Sietsma, Microstructural features of austenite formation in C35 and C45 alloys, Metallurgical and Materials Transactions 38 A (2007) 946-955.
[37] B. Pawłowski, Critical temperatures in steel, Monographs, AGH University of Science and Technology Publishing House, Cracow, 2012 (in Polish).
[38] T.C. Tszeng, G. Shi, A global optimization technique to identify overall transformation kinetics using dilatometry data – applications to austenitization of steels, Materials Science and Engineering 380 A (2004) 123-136.